Geoarchaeology

# New insights on the Monte Fenera Palaeolithic (Italy): Geoarchaeology of the Ciota Ciara cave



| | |
|---|---|
| Journal: | *Geoarchaeology* |
| Manuscript ID | Draft |
| Wiley - Manuscript type: | Research Article |
| Date Submitted by the Author: | n/a |





| | |
|---|---|
| Complete List of Authors: | Angelucci, Diego; Universita degli Studi di Trento Dipartimento di Lettere e Filosofia,<br>Zambaldi, Maurizio; Universita degli Studi di Trento Dipartimento di Lettere e Filosofia<br>Tessari, Umberto; Universita degli Studi di Ferrara, Dipartimento di Fisica e Scienze della Terra<br>Vaccaro, Carmela; Universita degli Studi di Ferrara, Dipartimento di Fisica e Scienze della Terra<br>Arnaud, Julie; Universita degli Studi di Ferrara, Dipartimento di Studi Umanistici<br>Berruti, Gabriele; Universita degli Studi di Ferrara, Dipartimento di Studi Umanistici<br>Daffara, Sara; Universita degli Studi di Ferrara, Dipartimento di Studi Umanistici<br>Arzarello, Marta; Universita degli Studi di Ferrara, Dipartimento di Studi Umanistici |
| Keywords: | Middle Pleistocene, Late Pleistocene, Middle Palaeolithic, cave-site, archaeological soil and sediment micromorphology |
| | |

# NEW INSIGHTS ON THE MONTE FENERA PALAEOLITHIC (ITALY): GEOARCHAEOLOGY OF THE CIOTA CIARA CAVE

Diego E. Angelucci (1,*), Maurizio Zambaldi (1), Umberto Tessari (2), Carmela Vaccaro (2), Julie Arnaud (3), Gabriele L.F. Berruti (3), Sara Daffara (3) & Marta Arzarello (3)

(1) Dipartimento di Lettere e Filosofia, Università di Trento, Italy; (2) Dipartimento di Fisica e Scienze della Terra, Università di Ferrara, Italy; (3) Dipartimento di Studi Umanistici, Università di Ferrara, Italy;
(*) Corresponding author: Dipartimento di Lettere e Filosofia, Università di Trento, via T. Gar 14, I-38122 Trento (Italy), tel.: +39 0461 282700 [mobile phone: +39 339 8047514], email: diego.angelucci@unitn.it

**ABSTRACT.** *Monte Fenera is a mostly carbonate-built hill at the southern border of Western Alps. It hosts several archaeological sites, among them karstic caves bearing evidence of Palaeolithic occupations. These sites have a long history within Alpine archaeology – having been explored since the 19th century – but information on their stratigraphy, chronology and formation remains incomplete. They are among the few cave-sites prior to the ALGM in the area, and their study is crucial for understanding human occupation and regional environmental evolution during the Pleistocene. Here we focus on Ciota Ciara, a cave formed in Triassic dolostone, and in particular on the geoarchaeological study of the succession unearthed at the cave entrance since 2009. The deposit dates from the Middle-Upper Pleistocene transition. Sediment accumulation was due to consecutive events of concentrated flow and runoff from the karstic system, alternating with episodes of wall disintegration and short phases of surface stabilization. Post-depositional processes include frost action, hydromorphism, and diagenesis that have selectively affected the archaeological remains. The results of the study elucidate site formation and have relevance for Pleistocene cave archaeology in the southern Western Alps.*

**KEY WORDS.** Middle Pleistocene, Upper Pleistocene, Middle Palaeolithic, cave-site, archaeological soil and sediment micromorphology

## 1. INTRODUCTION

Current data on human presence pre-dating the Würmian glaciation along the southern margin of the Alps are uneven, and almost absent for the central and western sides of the Alpine arc. This area (which corresponds to the Alpine and Prealpine sectors of the Italian regions of Piedmont and Lombardy) seems an empty patch within the relatively rich record of its macro-regional context. Lower and early Middle Palaeolithic sites are known in southern France, Liguria, the eastern side of the Southern Alps and around the northern Adriatic Sea (see, e.g., Cauche, 2009; Valensi & Psathi, 2004) but are almost absent in the western and central areas of the Southern Alps. However, archaeological evidence pre-dating the Würmian cycle (i.e. before Marine Isotope Stage 4) does in fact exist in the region, but often comes from sites explored in the 19$^{th}$ or early 20$^{th}$ centuries lacking proper chronological and stratigraphic contextualisation, or consists of surface- and stray-finds from open air-sites. There is also a general absence of geoarchaeological studies (with few exceptions, such as the Bagaggera site – see Cremaschi et al., 1990). One of the aims of ongoing research in northern Italy is to fill this information gap regarding the Lower and early Middle Palaeolithic of the region, both by reconsidering archaeological sites that were excavated in the past, and collecting new data from fieldwork in order to provide an appropriate scientific base.

Monte Fenera, in the Italian region of Piedmont, is one of the most important archaeological complexes at the southern border of the Western Alps. Monte Fenera is a mostly carbonate-built hill that is home to several palaeontological and archaeological sites, among them karstic caves bearing evidence of Palaeolithic human occupation. Ciota Ciara (meaning “bright cavern” in local dialect) is one of Monte Fenera’s cave-sites (Fantoni, Cerri, & Dellarole, 2005).

Fieldwork at Ciota Ciara was restarted in 2009 by a research team led by the University of Ferrara and has included the reopening of old test-trenches, as well as the stratigraphic excavation of new sectors. The latter have been explored by means of state-of-the-art archaeological methods and studied through an interdisciplinary approach, including geoarchaeological analysis, in order to understand site stratigraphy, site formation and archaeological assemblage integrity.

We here report on the first results of the geoarchaeological study of the Ciota Ciara cave and discuss their broader archaeological implications, focussing on the archaeological succession that was unearthed at one of the cave entrances.

## 2. THE CIOTA CIARA CAVE: SITE PRESENTATION

### 2.1. History of research

Ciota Ciara cave (Fig. 1) is located on the west slope of Monte Fenera at an altitude of 665 metres a.s.l., in the Borgosesia municipality (Vercelli), and is the only systematically excavated Pleistocene site in the Piedmont region (Italy). The data collected from Ciota Ciara provide clues for understanding the behavioural strategies and environmental context of Pleistocene hominins.

The Ciota Ciara cave, like many of the Monte Fenera sites, has long been known and explored. Previous campaigns at the cave uncovered Middle Palaeolithic lithic assemblages that were assigned to the so-called "Alpine Mousterian" (Battaglia, 1953; Lo Porto, 1957), a concept that has biased the interpretation of Neanderthal lithic assemblages in north-western Italy for a long time. Recent data on the archaeological assemblages of Ciota Ciara have led to the integration of the lithic productions collected at Monte Fenera within the Italian Middle Palaeolithic tradition, underlining at the same time the role of the raw material as far as the characteristics and morphology of lithic blanks are concerned.

Earlier excavations at Ciota Ciara cave date from the 1930s, when a first report on a non-systematic test-pit was published (Conti, 1931). The first proper survey of the cave was performed in 1953 by the local speleological association, while the earliest 'systematic' fieldwork dates from 1964 (Fedele, 1966; Strobino, 1992). During the 1960s and 1970s a few sporadic digs were undertaken in the cave, mainly by Francesco Fedele (see Fedele, 1984), while extensive exploration of the upper layers found at the cave entrance was carried out between 1991 and 1993 under the Italian Ministry of Culture (Busa, Gallo, & Dellarole, 2005). Archaeological assemblages collected during earlier campaigns were stored in the local museum at Borgosesia, often unlabelled and without any indication about their provenance. For this reason, the information that could be obtained from previously-collected remains was limited, and the study of Ciota Ciara cave had to start again from scratch. Research was resumed

in 2009 under the direction of the University of Ferrara, and regular excavation campaigns have been conducted at the site since then.

### 2.2. Geological and geomorphological context

Monte Fenera (maximum elevation 899 m a.s.l.) stands isolated at the foot of the western Alpine relief, on the left side of River Sesia (Fig. 1), at the border between the Alpine chain and the subsidence basin of the Po Plain (Fantoni, Decarlis & Fantoni, 2005). Monte Fenera is quite unusual as far as its geology is concerned: the Western Alps are mostly composed of igneous and metamorphic rocks, while the Monte Fenera include sedimentary, often carbonatic, strata. For this reason, the Monte Fenera is one of the few massifs of the western Alpine arc where karstic caves occur: due to its geological and geomorphological features, the Monte Fenera has attracted the attention of researchers since the 19$^{th}$ century (see Fantoni et al., 2005 for details).

Geologically, the Monte Fenera succession lies almost horizontally over the metamorphic basement (the "Serie dei Laghi"). From bottom to top, the following main geological formations are identified (Fantoni & Fantoni 1991; Berra et al., 2009; Beltrando et al., 2015): Permian Volcanic Complex (lava, tufa and other volcanic or pyroclastic rocks, 100-200-m-thick); Triassic grey \ green sandstone (mostly quartzarenite), with intercalations of pelite and doloarenite ( "Fenera Annunziata Sandstone" formation, few metres thick); *ca.* 300-m-thick succession mostly consisting of dolostone, with thin intercalations of clay, dolorudite and thin volcanoclastic horizons, dating from the Middle Triassic ("San Salvatore Dolomite" formation). A stratigraphic hiatus marks the Upper Triassic, while the Jurassic is represented by a thin basal unit of limestone \ dolomite breccia ("Brecce del Monte Fenera"), covered by a Sinemurian formation of sandstone and microconglomerate ("San Quirico Sandstone", 25-60-m-thick) and by the thick (*ca.* 250 m) Pliensbachian layers of the "Calcari spongolitici" formation, which consist of limestone with chert nodules and lenses (mostly spongolite) and intercalations of sandstone.

Present climatic data for the nearby town of Borgosesia indicate a mean annual temperature of *ca.* 11 °C and mean annual rainfall of about 1000 mm/a (data from www.arpa.piemonte.gov.it, download 12 December 2017).

### 2.3. Cave morphology

The nature of the Mesozoic succession and its geological setting have controlled the development of Monte Fenera's karstic network. More than seventy karstic caves are reported in Monte Fenera, mainly along its west slope. The formation of the karstic network probably dates from the Pliocene or the Messinian, even if its full development took place in the Quaternary (Fantoni & Fantoni, 1991; Bini et al., 2005). The caves are found within the "San Salvatore Dolomite" formation, due to the permeability barrier of the underlying volcanic complex – the only exception being the "Grotta dell'Arenaria", modelled in the "San Quirico Sandstone" formation. Most karstic cavities have developed along two main directions (ENE-WSW and NNW-SSE), roughly parallel to the Cremosina and Colma tectonic lines (Fantoni et al., 2005).

Ciota Ciara is an active karstic cave; it has a maximum length of about 80 m along its main axis and a depth of 15 m (that is, a positive difference in elevation from its lower entrance). The cave has two entrances (Fig. 2): the lower, at 665 m altitude a.s.l., faces south-west and corresponds to the area currently investigated by archaeological fieldwork; the upper (named "the window") is located at 670 m elevation a.s.l., faces west and has been artificially enlarged by the removal of boulders fallen from the cave ceiling. The cave's main passage runs NE-SW and is linked to the upper entrance by a short passage; a large hall ("sala") has formed at the intersection of these two passages. A lateral system of shafts can be accessed from the south-western entrance, leading to inner cavities at higher elevations ("Sala dei pipistrelli" and "Sala della torre"; Testa, 2005). After heavy rainfalls, vadose water may flow from both the main NE-SW passage and the second system, springing from the lower entrance.

### 2.4. Archaeological background and dating

The interdisciplinary study of the archaeological assemblages collected since 2009 at Ciota Ciara has yielded information on technical features, raw material supply, palaeoenvironment and the site's biochronology.

The raw materials employed to produce lithic artefacts are mainly pegmatitic quartz and, subordinately, chert (often spongolite from the "Calcari spongolitici" formation); they were both collected from the surroundings of the cave. Technological reduction sequences can be defined as typical Middle Palaeolithic and include multidirectional (opportunistic), discoid and Levallois methods. Retouched tools are relatively scarce at Ciota Ciara, perhaps as a result of the physical characteristics of the raw material; they mostly consist of side-scrapers and denticulated tools. Use-wear analysis shows that the activities carried out at the site were mostly related to food processing and wood working (Arzarello et al., 2012; Daffara et al., 2014; Angelucci et al., 2015; Buccheri et al., 2016).

In the 1980s, two isolated teeth and one fragment of temporal bone were found in the reworked sediment outside the cave and were assigned to *Homo neanderthalensis* (Mottura, 1980; Villa & Giacobini, 1993). The human remains have not yet been re-analysed and information on their specific morphology and on the reliability of the identification is not available.

The macro-mammal assemblage is dominated by remains of cave bear (*Ursus spelaeus*), which accounts for more than 80% of the faunal assemblage. Some of the *Ursus spelaeus* remains were modified by humans as they show cut marks probably associated with skinning activity (Buccheri et al., 2016), although most of them result from the natural deaths of animals that hibernated in the cave for lethargy. In all, a number of carnivore species were found (*Ursus arctos, Panthera leo spelaea, Panthera pardus, Lynx lynx, Canis lupus, Vulpes vulpes, Meles meles* and *Martes martes*), while the most common species of herbivores are *Rupicapra rupicapra, Cervus elaphus, Stephanorhinus* sp. and *Bos* sp. (Angelucci et al., 2015; Buccheri et al., 2016). The small-mammal assemblage shows great diversity and is dominated by *Clethrionomis glareolus* and *Pliomys coronensis*. Palaeoecological indicators suggest a change from a relatively cold, humid environment in the lower layers of the deposit to warmer but still humid conditions in the upper ones. Furthermore, the presence of *Pliomys coronensis* attests that the cave was occupied during a relatively warm phase (Berto et al., 2016). Preliminary numerical dating results for the Ciota Ciara deposit indicate that it may date from the second half of the Middle Pleistocene (pers. comm. J.J. Bahain and A. Vietti, 2016).

## 3. MATERIALS AND METHODS

The study of Ciota Ciara has been undertaken using a 'classical' geoarchaeological approach, since no previous data were available. Research procedures and data collection included accurate field description and sampling, followed by routine sedimentological analyses, basic geochemical characterisation (still ongoing and not reported in this paper) and soil micromorphological observation.

The first stage of the study was the systematic description and drawing of all sections exposed during the 2009 and 2016 field campaigns. The sections and extant excavation surfaces were described in detail, taking into account sedimentary, soil, stratigraphic and archaeological features, in order to identify geoarchaeological field units (as defined in Angelucci, 2002).

All the units were sampled (see below and Table I): twenty-two bulk samples were collected from the site (18 samples) and from its surroundings (4 samples) for sedimentological analyses. Routine sedimentological analyses were performed at the laboratories of the Department of Physics and Earth Science of the University of Ferrara. After appropriate preparation, all the samples were analysed to obtain grain size distribution and textural classification by means of instruments based on Stokes Law (settling tube for sand fraction and Micrometrics Sedigraph for mud). The data are expressed according to the Wentworth (1922) classification, while textural parameters were calculated following Folk and Ward (1957). Organic matter content was evaluated by Loss on Ignition (LOI), according to the procedure proposed by Heiri et al. (2001), while calcium carbonate content was determined using an electronic gas-volumetric calcimetre.

Eight samples for soil micromorphology were collected during the 2014 and 2016 field seasons. Undisturbed samples were removed by simple extraction (thanks to the good cohesion of the sediment), wrapped in paper, marked, and oven-dried at 60°C until a constant weight was attained. Thin sections were prepared at IPHES (Institut de Paleoecologia Humana i Evolució Social, Tarragona, Spain) and "Servizi per la Geologia" laboratories (Piombino, Italy), in the following stages: impregnation with a mixture of resin, styrene, and hardener; curing; cutting into cm-thick slabs; and final preparation of 25-mm sections, measuring 95 mm by 55 mm. Thin sections were

examined at the University of Trento under a polarizing microscope at magnifications between 20x and 1000x, using plane-polarized light (PPL), cross-polarized light (XPL) and oblique incident light (OIL), the last for primary fluorescence observation using two distinct wideband filter combinations (ultraviolet and blue light). Images were recorded using a digital camera for polarizing microscopy. Thin-section description follows the guidelines proposed by Stoops (2003), with integrations after Brewer (1976), namely for the use of the terms 'pedorelicts' and 'papules', and after Nicosia & Stoops (2017).

## 4. THE SUCCESSION AT THE CIOTA CIARA ENTRANCE

### 4.1. Stratigraphic layout and field characteristics

The infilling of the south-western entrance of the Ciota Ciara cave is the remnant of a thicker stratification that was removed during earlier campaigns. According to the available information, the upper part of the deposit was composed of reworked sediment and contained mixed archaeological assemblages. Five excavation units were identified during current fieldwork. The units dip outwards with a low angle and have slightly irregular stratigraphic boundaries (see Fig. 3 – the systematic description of the field characteristics can be found in Table II).

Field observation showed that some units include more than one facies; for this reason, the units were divided into sub-units (see Table II). All the units are badly-sorted sandy-silt to silty-loam, reddish-brown to brown, massive and chaotically-arranged, with common to many stones (mostly fragments of local dolostone, with subordinate fragments of sandstone from the San Quirico Sandstone formation and occasional exotic components – see below). Thin intercalations of well-sorted sand occur within layers 13 and 14. Concentrations of Fe-Mn oxides, phosphatic rinds and textural coatings are ubiquitous. Archaeologically, unit 14 is particularly rich, and unit 15 contains both lithic and faunal remains as well; unit 16 has not yielded any archaeological evidence so far.

Unit 13 is silty-clay with few stones (dolostone fragments, most of them weathered), brown-coloured with black staining due to secondary Fe-Mn oxide accumulation. The layer shows slight traces of past biological activity related to insects nests and root action, which has probably masked former internal

flat lamination, locally still recognized. Unit 13 lays on layer 14 with a poorly distinct, gradual, apparently horizontal boundary.

On average, unit 14 is silty-loam with frequent to many stones and includes distinct, well-recognized sub-units (Table II). The unit dips south-west and exhibits lateral variations in the shape, size, weathering and arrangement of the coarser, dolostone fragments. Traces of biological activity are scarce and related to root action. The lower boundary to layer 15 is poorly distinct, marked by an increase of dolostone fragments (sometimes arranged as a sort of discontinuous stone-line) and sand fraction.

Unit 15 is a clast-supported breccia with fine sand- to silty-loam massive matrix filling all pores. Coarse components include dolostone fragments from the cave roof and walls; their average size decreases from top to bottom. The bottom layer, unit 16, is similar to unit 15 as far as its sedimentary characteristics are concerned (but with slightly larger stones) and rests on cave bedrock.

**4.2. Sedimentological analyses**

Fifteen bulk samples collected from units 13, 14, 15 and 16 were analysed to obtain grain-size distribution and textural classification of the fine earth (see chapter 3). Results show that all the units are composed of poorly-sorted sandy-silt or silty-loam sediment. Data from textural analyses are plotted as cumulative curves for each unit (Fig. 4). Organic matter content was determined by means of Loss on Ignition (LOI) analysis (Fig. 5). The quantity of organic matter ranges from *ca.* 3% to 6% across the succession; no relevant variations are observed within the deposit. Calcium carbonate content is low in all the units (Fig. 5).

**4.3. Archaeological micromorphology**

Under the microscope, the thin sections from units 13 and 14 of Ciota Ciara show clear similarities, with the exception of the samples from sub-unit 14c and unit 15, which exhibit some differences. Coarse constituents are fairly homogeneous and ubiquitous throughout the succession. They have been clustered into four main groups (Table III).

Siliciclastic fraction (SIL). These components are mostly included in the silt and sand fractions and consist of mineral and rock fragments as follows (in order of abundance): common angular to subangular monocrystalline quartz, sometimes with wavy extinction pattern; common chert fragments (mostly spongolite, subordinately radiolarite – single spicules or radiolarians are often observed within the groundmass), from angular to subrounded (Fig. 6: A, B and F); few angular to subangular feldspars (both alkaline feldspars and plagioclase) and micas (mostly muscovite, subordinately biotite); very few, mostly subangular sandstone fragments, derived from the San Quirico Sandstone formation (see above). This class also includes the "exotic pebbles" (see below), fragments of igneous or metamorphic rocks that occur as small rounded pebbles or granules (Fig. 6: C and D).

Carbonate components (CRB), which include two constituents: common angular and subangular, heterometric (from few mm- to cm-sized) dolostone and limestone fragments from the San Salvatore Dolomite formation (Fig. 6: E), sometimes with traces of physico-chemical weathering; common angular calcite/dolomite crystals, which derive from the disintegration of the local dolostone (the term "calcite/dolomite" is used here as these minerals are not easily distinguished under the optical microscope). Both components come from the cave roof and walls, although they may have been affected by short-distance transport from the inner part of the cave.

The components related to biological activity or human inputs have been clustered under the class "anthropogenic and biogenic components" (ABC), which include: bone fragments (from tens-of-µm- to mm-sizes), showing different degrees of physical weathering, as well as presence of Fe-Mn oxide coatings (Fig. 7: A and B; see below) and, occasionally, evidence of thermal impact (Fig. 7: C and D); subangular to subrounded fragments of phosphatic composition, mostly amorphous and with undifferentiated b-fabric, strongly fluorescent under BL; few excrements (Fig. 7: C and D), sometimes from carnivores; occasional small charcoal fragments of vegetal origin; rare knapped lithic artefacts (an example is given by the chert microflake depicted in Fig. 6: F – see also Angelucci, 2010).

The "other components" cluster includes 'pedorelicts' and 'papules' (respectively fragments of older soils and reworked clay coatings embedded in the groundmass, see Brewer, 1976), which derive from

the erosion of pre-existing soil covers that were in-washed into the cave network and transported by the karstic water.

Units 13 and 14 reveal similar characteristics as far as their composition, microstructure and pedofeatures are concerned: both the units show complex, heterogeneous, silty-clay groundmass, and contain intercalations of distinct facies, such as the sand levels detected in units 13, 14b and 14c – Fig. 7: E and F). The variety of facies observed at the macroscopic scale within unit 14 (see Table II) has been fully confirmed by microscopic observation.

The fine material of units 13 and 14 is brown, and a slight prevalence of fine over coarse material is observed (c/f limit at 4 μm); c/f related distribution pattern is mostly single- to open-porphyric; b-fabric ranges from undifferentiated to locally granostriated (Tables III and IV). Across the units, microstructure changes progressively from top to bottom, namely from weakly-developed subangular blocky to moderately-developed platy. Locally, evidence of biological activity such as root action and insect nesting is observed, with occurrence of channel and spongy secondary microstructures (e.g. in the sub-units 13 and 14a). Unit 14c exhibits single- to bridged-grain microstructure: in the field, this unit consists of a set of fine sand and silt layers affected by sedimentary deformation structures (see Table II).

Pedofeatures are also similar across units 13 and 14 (Table IV). Secondary accumulations of Fe-Mn oxides (see, e.g., Fig. 8: A) are detected in form of nodules, coatings and hypocoatings: irregular intrapedal typic, sometimes dendritic, impregnative nodules are ubiquitous; coatings and hypocoatings are mostly developed around bone fragments and phosphatic components (Fig. 7: A and B), while only a few are found around mineral grains or in planes and channels. The local occurrence of bleached, greyer fine material in sub-units 14f and 14e points to the partial depletion of the Fe-Mn oxide due to short-distance segregation under alternating redoximorphic conditions (see, e.g., Lindbo, Stolt & Vepraskas, 2010: 137-138). Secondary phosphate accumulation and impregnations (see, e.g., Karkanas, 2001) are widespread in all the units but unevenly distributed, and affect many components – especially weathered bone fragments (Fig. 8: B). The observed phosphatic pedofeatures are (in order of abundance): subrounded and amorphous strongly impregnated nodules, coatings and hypocoatings around some fragments of carbonate rocks, and reaction rims related to the interaction between

calcium carbonate and phosphate (Fig. 8: C and D). Textural pedofeatures are common as well and include: (a) discontinuous brown or orange clay coatings on mineral grains and rock fragments (Fig. 6: A and B), observed in all the units; (b) orange or yellow limpid, locally dotted, clay coatings (locally forming infillings), sometimes slightly deformed and fragmented (e.g. in sub-units 14a, 14b and14e – see Fig. 7: C); (c) yellowish brown silty clay coatings along voids walls (sub-units 13, 14a and 14b – see Fig. 8: E and F); (d) inherited and disrupted clay coatings, along with clay 'papules', locally microlaminated and randomly distributed inside the groundmass (sub-units 14f and 14e); (e) very few clay intercalations (e.g. sub-unit 14b – Fig. 7: E and F). The widespread presence of the textural pedofeatures across all the facies suggests that several phases of clay migration took place and affected the whole thickness of the deposit. Finally, a few loose discontinuous infillings are observed inside channels and locally planes; some of them are clearly biogenic, while others are composed of random distributed silt- to sand-sized grains of calcite/dolomite, chert and quartz (Fig. 8: E and F). The origin of the latter is not clear yet: they may result from frost action, injection (Van Vliet-Lanoë, 2010) or other post-depositional processes.

As observed in the field, unit 15 differs from the upper layers. The unit exhibits clear evidence of frost action related to freeze/thaw (Van Vliet-Lanoë, 1985; 2010). The main characteristics attesting to frost action are (Fig. 9): (a) the platy, locally banded, microstructure; (b) the widespread occurrence of silt cappings on rock fragments; (c) the presence of common, randomly distributed, disrupted and reworked clay coatings. Phosphate coatings and nodules are also detected in unit 15 (see Tables III and IV), and the groundmass is enriched in phosphate.

During fieldwork at Ciota Ciara, a great variability in the size, shape and degree of weathering of the bone fragments and in the occurrence of Fe-Mn oxide staining on them was observed: the same variability was detected under the microscope. A semi-quantitative approach was thus applied in order to estimate the relationships between the size of the bone fragments, their degree of weathering and the development of Fe-Mn oxide coatings. The bone fragments visible in the thin sections from units 13, 14 and 15 (with the exception of sub-unit 14c) were totalled taking into account two size-classes: between 60 and 500 µm (that is, equivalent to very fine, fine and medium sand) and larger than 500 µm. The gross total includes *ca.* 600 bone fragments (see Fig. 10). For each bone fragment, the

following parameters were recorded: degree of physical weathering (scaled as: low, moderate, intense); occurrence and development of Fe-Mn coatings on the bone surface (absent, less than 50%, more than 50%); and degree of thermal impact (absent, low, intense).

The relationship between the size of the bone fragments, their degree of weathering and the occurrence of Fe-Mn oxide coating looks diagnostic (Fig. 10). A moderate positive correlation between the degree of weathering and the presence of Fe-Mn oxide pedofeatures is detected in units 13 and 14 (respectively, 40% and 64% of the bone with intense weathering is coated with Fe-Mn oxide) and becomes strong in unit 15 (+90% of the bones with intense weathering has continuous coatings, while this correspondence is less than 50% for bone with low or moderate alteration). At the same time, the correlation between the size of the bone and the occurrence of Fe-Mn coating is clearly positive in all the units. In unit 13, most of the bone fragments smaller than 500 µm show partial or intense weathering but absence of Fe-Mn coatings; on the contrary, the coatings are well-developed around the larger pieces (see data in Fig. 10). The same positive trend also exists in unit 14, in which almost 90% of the larger bones are Fe-Mn-coated, and in unit 15.

## 5. DISCUSSION

Despite the shallowness of the deposit and the lack of proper contextualisation, the analysis of the Ciota Ciara succession is significant, given the scarcity of reliable data on the human occupation of the southern Western Alps before the Würmian glaciation. As emphasized above, evidence of human occupation dating from the Early and Middle Palaeolithic does exist in this area; what is missing is a modern, sound scientific approach. The current project at Monte Fenera is an initial attempt to provide such an approach.

### 5.1. Stratigraphic layout

Its stratigraphic layout (see Fig. 3) and sedimentary characteristics indicate that the deposit filling the Ciota Ciara south-western entrance came from the cave and that it was laid down by dynamics related to concentrated flows from the inner karstic system, in association with the accumulation of rock

fragments from the disintegration of the cave walls and roof. Occasional deposition events by surface water currents through tractive mechanisms are also detected, as well as short phases of surface stabilization. In fact, the present cave entrance functioned as a 'cave exit', that is, a point of emergence of karstic water – most probably a free draining spring controlled by the permeability boundary underneath the "San Salvatore Dolomite" formation which hosts the karstic system. This type of spring is fairly common in karstic systems (see, e.g., Ford & Williams, 2007). The archaeological implications of the depositional dynamics are important, since part of the collected assemblages has undergone short-distance displacement (see below)

The stratigraphy of the deposit points to an accumulation formed by consecutive events, although the lack of major discontinuities within the succession suggests that it was probably laid down at a regular pace. At the same time, the vertical distribution of microstructures and certain other characteristics (in particular those related to soil reworking or in-wash, such as the fragmented pedofeatures, the 'pedorelicts' and 'papules', see chapter 4.3) reveal a gradual change in the post-depositional processes, which may result from climatic fluctuations through time.

**5.2. Sedimentary sources and dynamics**

The coarse components observed in the deposit (see chapter 4.3) come from distinct sources. The carbonate constituents (CRB) derive from the roof and walls of the cave entrance or from short-distance reworking from the inner cave passage (see Fig. 2). They include rock fragments and isolated crystals of calcite/dolomite from mechanical breakage of pre-existing rock fragments. The origin of the siliciclastic fraction (SIL) is varied. Most of it comes from the Mesozoic sedimentary formations which feed the upper part of the Ciota Ciara karstic network: the chert fragments are from the "Calcari spongolitici" formation; the sandstone fragments belong to the "San Quirico Sandstone"; the same formation is the primary source for the quartz, feldspar and mica grains, and for the occasional amphiboles and pyroxenes (these minerals are basic components of the sandstone – see Beltrando et al., 2015). Yet it cannot be excluded that a part of the siliciclastic fraction may primarily derive from aeolian inputs, as well-rounded, polished grains of quartz and feldspar were detected under the microscope. At the same time, it is not possible to gauge the inputs from former surface sediments or

soil covers outcropping on Monte Fenera's slopes that could have been washed into the cave system and transported by karstic waters – although input from former soils is demonstrated by the presence of 'pedorelicts' and 'papules' (see Fig. 9). Data on soils and surface sediments on the slopes of Monte Fenera are almost non-existent, and further analyses are needed in order to provide reliable information on these inputs.

Among the components detected both in the field and under the microscope at Ciota Ciara are the "exotic pebbles" ("ciottoletti esotici", in Italian – see Fig. 6: C and D). These are well-rounded pebbles and granules of mafic or ultramafic igneous (mostly amphibolite) and metamorphic rocks (often quartzite or gneiss), systematically found in the cave infillings of Monte Fenera. During 20$^{th}$ century excavation campaigns, the "exotic pebbles" often attracted the attention of archaeologists, and their origin has been much debated. Monte Fenera was never reached by Alpine glaciers during the Pleistocene, but an explication of pebbles' origin is given by Fantoni & Fantoni (1991): they are remnants from the erosion of the Miocene sedimentary cover that is found all along the Southern Alps, but that has largely been washed away as a result of tectonic uplifting and subsequent erosion during the Pliocene and Pleistocene.

The group of anthropogenic and biogenic components (ABC) includes several distinct categories. Constituents such as the charcoal fragments, probable lithic artefacts (see Fig. 6) and burnt bone fragments are anthropogenic. Other components such as the excrements (of variable origin, from both herbivores and carnivores) and the unburnt bone fragments may be of purely biogenic origin. While the other components of this class are rather scarce, the bone fragments are common, and the variety of their characteristics is a diagnostic feature with respect to the origin and post-depositional history of the biogenic \ anthropogenic fraction.

The bone fragments observed under the microscope show distinct features: some bone fragments show the effects of heating (a marker for human impact); some are greatly reduced in size (tens of microns), but without any evidence of weathering or secondary impregnation by phosphate (their origin is unclear and could be related to trampling, crushing or other process); some others are greatly reduced in size and show evidence of weathering and secondary impregnation by phosphate, and sometimes traces of degradation by biological agents (they may derive from digestion, excrements or owl \ other

avian pellets – see, e.g. Fig. 8); lastly, many bone fragments are stained or coated by secondary precipitates of Fe-Mn oxides. Quantitative analysis of the relationships between the size of the bones, their degree of weathering and the development of Fe-Mn-oxide coating has shown the existence of a positive correlation (see chapter 4.3): the larger the bone fragment, the more developed the Fe-Mn oxide coating (in all the units); the more weathered the bone, the more developed the coating (in particular in unit 15). These data show that the bones collected from units 14 and 15 do not belong to a homogeneous assemblage – that is, some were discarded at the cave entrance and were found in almost their original position, while some have undergone short-distance displacement from the cave to its entrance, as also attested by the distinct taphonomy of bear remains (Buccheri et al., 2016). Sedimentary dynamics are difficult to establish under the microscope, as original fabrics are often masked by the 'pedogenic' microstructure: field evidence is more diagnostic. According to field data (see chapter 4.1), most units possess the characteristics of slope sediments related to mixed dynamics (meaning gravity associated with water flow), with intermediate to high sediment concentration (see Bertran & Texier, 1999). All the units show chaotic, massive, random arrangements related to poorly-selective accumulation dynamics such as debris- or mud-flow, with the exception of the few intercalations (such as sub-unit 14c) that were laid down by runoff or other tractive mechanisms by the karstic water emerging from the cave.



**5.3. Post-depositional processes**

Post-depositional processes include frost action, hydromorphism, secondary accumulation of soluble substances, as well as weathering dynamics and diagenesis that have selectively affected both natural and archaeological components.

The secondary accumulation is mainly related to phosphate, that has accumulated in the form of nodules and coatings \ hypocoatings on the carbonate components (see Fig. 8). The intensity of the diagenetic phosphate accumulation increases from bottom to top, due to outcropping of bedrock below units 15 and 16 and consequent restricted water infiltration in the lower part of the deposit. The accumulation of Fe-Mn oxide is ubiquitous and gave rise to nodules, intercalations and coatings, in particular on the bone fragments (see above): the nodules and intercalations point to redoximorphic

conditions within the sediment due to the temporary occurrence of a perched water-table related to the permeability barrier at the boundary between unit 16 and the bedrock.

The action of discontinuous frost could be recognised at the base of unit 14 and within unit 15, due to the platy microstructure and the presence of cappings (see Fig. 9). The frost-related features are not observed in unit 13 and in the upper part of unit 14.

The distribution and characteristics of post-depositional features help in understanding the morphology of the cave entrance during human occupation. Some of the post-depositional dynamics detected can be related to diagenesis (for instance, clay translocation or the secondary accumulation of Fe-Mn oxides) and are not distinctive of proper soil formation. Nevertheless, other features indicate that the deposit was exposed to soil-forming-like dynamics soon after its accumulation. The main markers for exposure to external, subaerial conditions are the development of microstructure and the frost-related features detected in the lower part of the succession – the latter indicating that the deposit was affected by temperature fluctuations, usually not observed inside deep caves. These data suggest that the slope and the cave dripline have not significantly retreated since the Pleistocene human occupation, or that the recession has been negligible.



**5.4. Final remarks**

The geoarchaeological study of the deposit infilling the south-western entrance of Ciota Ciara has enabled the understanding of archaeological site formation and a reassessment of its significance, in particular with respect to human Pleistocene occupation of the southern Western Alps, a region in which the archaeological evidence pre-dating the Würmian glaciation needs to be re-evaluated.

The data presented here show that the infilling of the entrance was mainly built up by debris-flow and runoff events coming from the cave's internal passage. This evidence, associated with the examination of differential weathering of the remains and distribution of the pedofeatures (in particular Fe-Mn oxide coatings and stains), demonstrates that only a part of the assemblage collected at the cave entrance is *in-situ*: another part was transported from the passage that feeds the entrance. For this reason, accurate analysis of the faunal remains taphonomy and of the lithic artefact wear traces is needed in order to evaluate the integrity of the archaeological assemblage. Future geoarchaeological

analyses of the deposits preserved within the cave may help in understanding the exact dynamics of site formation.

The archaeological micromorphology results show that the lower part of the examined succession suffered significant frost action soon after its accumulation. A previous study based on the palaeoecology of mammal assemblages suggested that the cave was occupied during a temperate phase and dated the upper part of the deposit to Marine Isotope Stage 5, that is, to the last Interglacial (Berto et al., 2016). In addition, palaeoecological indicators suggested a relatively cold environment for the lower portion of the succession: this is fully confirmed by the geoarchaeological data. It is thus likely that the lower part of the succession, in particular unit 15, date from the Middle Pleistocene, as preliminary numerical dating results suggest (pers. comm. J.J. Bahain, 2016). These data indicate that the Ciota Ciara deposit covers a time-span corresponding to the transition between the Middle and the Upper Pleistocene.

The application of geoarchaeological techniques to the study of Ciota Ciara has shown that this cave still bears important information for the Pleistocene archaeology of the Alpine region, despite the absence of data from previous excavation campaigns. The extensive revision of the chronological and stratigraphic data from the other Palaeolithic sites on Monte Fenera and in the surrounding area will be critical for our comprehension of the patterns of human occupation of the Alpine region.



**ACKNOWLEDGMENTS**

Archaeological fieldwork and research at Ciota Ciara is conducted in collaboration with the *Soprintendenza Archeologia, Belle Arti e Paesaggio delle Province di Biella, Novara, Verbano-Cusio-Ossola e Vercelli* and funded by the Municipality of Borgosesia and the University of Ferrara. Maurizio Zambaldi is a doctoral grantee of the University of Trento. The authors are indebted to the GASB (Gruppo Speleologico di Borgosesia) for its assistance with fieldwork; to Erica Patauner for helping in microscopic observation; to the Geoarchaeology Research Unit of IPHES (Institut de Paleoecologia Humana i Evolució Social, Tarragona, Spain) and to the "Servizi per la Geologia" laboratories (Piombino, Italy) for thin sections preparation; to Amina Vietti and Jean-Jaques Bahain for providing preliminary information on dating; to Jim Bishop for carefully revising the English text.

## AUTHOR CONTRIBUTION STATEMENT

D.E. Angelucci, M. Zambaldi and M. Arzarello designed the research and wrote the paper; J. Arnaud, G. Berruti, S. Daffara and M. Arzarello directed fieldwork at the site; D.E. Angelucci, M. Zambaldi, U. Tessari and C. Vaccaro performed analyses; D.E. Angelucci, M. Zambaldi and U. Tessari analysed data.

## REFERENCES

Angelucci D.E. (2002). The Geoarcheological Context. In J. Zilhão & E. Trinkaus (Eds.), *Portrait of the Artist as a Child. The Gravettian Human Skeleton from the Abrigo do Lagar Velho* (pp. 58–91). Trabalhos de Arqueologia, 22. Lisboa: IPA.

Angelucci, D.E. (2010). The recognition and description of knapped lithic artifacts in thin section. *Geoarchaeology*, 25(2), 220-232.

Angelucci, D.E., Arnaud, J., Arzarello, M., Berruti, G., Berruto, G., Berté, D., Berto, C., Buccheri, F., Casini, A., Daffara, D., Luzi, E., Lopez Garcia, J.M., Peretto, C., & Zambaldi, M. (2015). L'occupazione musteriana della grotta della Ciota Ciara, nuovi dati dalla campagna di scavo 2014. *Quaderni della Soprintendenza Archeologica del Piemonte*, 30, 400–402.

Arzarello, M., Daffara, S., Berruti, G., Berruto, G., Berté, D., Berto, C., Gambari, F. M., & Peretto, C. (2012). The Mousterian Settlement in the Ciota Ciara Cave: the oldest evidence of Homo Neanderthalensis in Piedmont (Northern Italy). *Journal of Biological Research*, 85, 71–75.

Battaglia, R. (1953). Le ossa lavorate della Caverna Pocala nelle Venezia Giulia e il problema del "Musteriano Alpino". *Bullettino di Paletnologia Italiana*, 63, 5–15.

Beltrando, M., Stockli, D.F., Decarlis, A., & Manatschal, G. (2015). A crustal-scale view at rift localization along the fossil Adriatic margin of the Alpine Tethys preserved in NW Italy. *Tectonics,* 34, 1927-1951.

Berra, F., Galli, M.T., Reghellin, F., Torricelli, S., & Fantoni, R. (2009). Stratigraphic evolution of the Triassic-Jurassic succession in the Western Southern Alps (Italy): The record of the two-stage rifting on the distal passive margin of Adria. *Basin Research*, 21, 335–353.

Berto, C., Bertè, D., Luzi, E., López-García, J. M., Pereswiet-Soltan, A., & Arzarello, M. (2016). Small and large mammals from the Ciota Ciara cave (Borgosesia, Vercelli, Italy): An Isotope Stage 5 assemblage. *Comptes Rendus - Palevol*, 15(6), 669–680.

Bertran, P. & Texier, J.-P. (1999). Facies and microfacies of slope deposits. *Catena*, 35, 99-121.

Bini, A., Zuccoli, L., Fantoni, R., Cerri, R., & Dellarole, E. (2005). Evoluzione del carsismo nelle Alpi. In R. Fantoni, R. Cerri, & E. Dellarole (Eds.), *D'acqua e di pietra. Il Monte Fenera e le sue collezioni museali* (pp. 143-152). Alagna Valsesia: Associazione Culturale ZEISCIU.

Brewer, R. (1976). Fabric and mineral analysis of soils. 2nd ed. New York: Robert E. Krieger.

Buccheri, F., Bertè, D. F., Luigi, G., Berruti, F., Cáceres, I., Volpe, L., & Arzarello, M. (2016). Taphonomic analysis on fossil remains from the Ciota Ciara cave (Piedmont, Italy) and new evidence of cave bear and wolf exploitation with simple quartz flakes by Neanderthal. *Rivista italiana di Paleontologia e Stratigrafia*, 122, 41–54.

Busa, F., Gallo, L. M., & Dellarole, E. (2005). L'attività di ricerca nelle grotte del Monte Fenera. In R. Fantoni, R. Cerri, & E. Dellarole (Eds.), *D'acqua e di pietra. Il Monte Fenera e le sue collezioni museali* (pp. 218–223). Alagna Valsesia: Associazione Culturale ZEISCIU.

Cauche, D. (2009). Les stratégies de débitage dans les industries lithiques archaïques des premiers habitants de l'Europe. *L'Anthropologie*, 113, 178–190.

Cremaschi, M., Fedoroff, N., Guerreschi, A., Huxtable, J., Colombi, N., Castelletti, L., & Maspero, A. (1990). Sedimentary and pedological processes in the Upper Pleistocene loess of northern Italy. The Bagaggera sequence. *Quaternary International*, 5(C), 23–38.

Conti, C. (1931). Valsesia Archeologica. Note per una sua storia dalle origini alla caduta dell'Impero Romano. *Bollettino della Società Storica Sudalpina*, 123, 1–61.

Daffara, S., Arzarello, M., Berruti, G. L. F., Berruto, G., Bertè, D., Berto, C., & Casini, A.I. (2014). The Mousterian lithic assemblage of the Ciota Ciara cave (Piedmont , Northern Italy): exploitation and conditioning of raw materials. *Journal of Lithic Studies*, 1, 1–16.

Fantoni, R., & Fantoni, E. (1991). Geologia del monte Fenera: ipotesi sulla genesi del sistema carsico. *De Valle Sicida*, 2(1), 11–22.

Fantoni, R., Cerri, R., & Dellarole, E. (2005). *D'acqua e di pietra. Il Monte Fenera e le sue collezioni museali*. Alagna Valsesia: Associazione Culturale ZEISCIU, 336 p.

Fantoni, R., Decarlis, A., & Fantoni, E. (2005). Geologia del Monte Fenera, In R. Fantoni, R. Cerri, & E. Dellarole (Eds.), *D'acqua e di pietra. Il Monte Fenera e le sue collezioni museali* (pp. 86-91). Alagna Valsesia: Associazione Culturale ZEISCIU.

Fantoni, R., Fantoni, E., Cerri, R., & Dellarole, E. (2005). Gli studi di Pietro Calderini sulla geologia del Monte Fenera. Il contributo scientifico dei ricercatori locali nell'Ottocento valsesiano. In R. Fantoni, R. Cerri, & E.

Dellarole (Eds.), *D'acqua e di pietra. Il Monte Fenera e le sue collezioni museali* (pp. 44–52). Alagna Valsesia: Associazione Culturale ZEISCIU.

Fedele, F. (1966). La stazione paleolitica del Monfenera (Borgosesia). *Rivista di Studi Liguri*, 32, 5–105.

Fedele, F. (1984). Il Paleolitico in Piemonte: Le Alpi Occidentali. *Ad Quintum. Archeologia del Nord-Ovest. Bollettino del Gruppo Archeologico "Ad Quintum" di Collegno (Torino),* 7, pp. 23-44.

Folk, R.L. & Ward, W.C. (1957). Brazos River bar: a study in the significance of grain size parameters. *Journal of Sedimentary Petrology*, 27, 3–26.

Ford, D. & Williams P. (2007). *Karst Hydrogeology and Geomorphology* [revised ed.]. Chichester: Wiley.

Heiri, O., Lotter, A.F., & Lemke, G. (2001). Loss on ignition as a method for estimating organic and carbonate content in sediments: reproducibility and comparability of results. *Journal of Paleolimnology*, 25, 101 –110.

Karkanas, P. (2001). Site formation processes in Theopetra Cave: a record of climatic change during the Late Pleistocene and Early Holocene in Thessaly, Greece. *Geoarchaeology, 16*(4), 373-399.

Lindbo, D.L., Stolt, M.H., & Vepraskas, M.J. (2010). Redoximorphic features. In G. Stoops, V. Marcelino & F. Mees (Eds.), *Interpretation of Micromorphological Features of Soils and Regoliths* (pp. 129-147). Amsterdam: Elsevier.

Lo Porto, G.F. (1957). Tracce del "Musteriano Alpino" in una grotta del Monfenera, presso Borgosesia. *Rivista di Studi Liguri*, 23, 286–293.

Mottura, A. (1980). Un frammento di osso temporale di tipo neandertaliano dalla grotta della Ciota Ciara. *Antropologia contemporanea*, 3, 373-379.

Nicosia, C, & Stoops, G., Eds. (2017). *Archaeological Soil and Sediment Micromorphology.* Chichester: Wiley.

Stoops, G. (2003). *Guidelines for analysis and description of soils and regolith in thin sections.* Madison: Soil Science Society of America.

Strobino, F. (1992). Nota sulla cronistoria delle ricerche sul Monte Fenera dalle origini agli anni sessanta, prospettive per le future indagini. *Periodico Annuale Società Valsesiana di Cultura*, 3, 7–14.

Testa, P. (2005). Il fenomeno carsico sul Monte Fenera. In R. Fantoni, R. Cerri, & E. Dellarole (Eds.), *D'acqua e di pietra. Il Monte Fenera e le sue collezioni museali* (pp. 152–163). Alagna Valsesia: Associazione Culturale ZEISCIU.

Van Vliet-Lanoë, B. (1985). Frost effects in soils. In J. Boardman, (Ed.), *Soils and Quaternary Landscape Evolution* (pp. 117-158). Chichester: Wiley.

Van Vliet-Lanoë, B. (2010). Frost Action. In G. Stoops, V. Marcelino, & F. Mees (Eds.), *Interpretation of micromorphological features of soil and regoliths* (pp. 81-108). Amsterdam: Elsevier.

Valensi, P., & Psathi, E. (2004). Faunal Exploitation during the Middle Palaeolithic in south-eastern France and north-western Italy. *International Journal of Osteoarchaeology*, 14, 256–272.

Villa G. & Giacobini G. (1993). Borgosesia, Monte Fenera. Denti neandertaliani dalla grotta Ciota Ciara. *Quaderni della Soprintendenza Archeologica del Piemonte*, 11, 300-303.

Wentworth, C.K. (1922). A scale of grade and class terms for clastic sediments. *Journal of Geology*, 30, 377–392.

**Captions of tables and figures** for the paper "NEW INSIGHTS ON THE MONTE FENERA PALAEOLITHIC (ITALY): GEOARCHAEOLOGY OF THE CIOTA CIARA CAVE", by Angelucci *et alii*

**Tables**

**Table I.** Ciota Ciara. List and number of analysed samples (see text for details). Key: TS –thin sections.
**Table II.** Ciota Ciara. Main characteristics of excavated units. Key: DP – distribution pattern; fr(s). – fragment(s); OP – orientation pattern.
**Table III.** Ciota Ciara. Main micromorphological characteristics (I): microstructure and components. Key: dev. – developed; fr(s). – fragment(s); mod. – moderately; coarse components are reported in order of abundance (see text for details).
**Table IV.** Ciota Ciara. Main micromorphological characteristics (II): groundmass and pedofeatures. Key: c/f RlDP – coarse/fine related distribution pattern; fr(s). – fragment(s); undiff. – undifferentiated.

**Figures**

**Figure 1.** Location (above) and view of Monte Fenera (below).
**Figure 2.** Ciota Ciara. Top right: sketch plan of the cave: solid line – outline of the cave wall; dashed line – dripline at the cave entrances; 1 – W entrance (the "window"); 2 – SW entrance in 2009 (before excavation). Bottom right: long-section of the cave (modified after Fedele, 1966).
**Figure 3.** Ciota Ciara. Stratigraphic cross-sections across squares F4-D4 (top) and D4-D2. Key: 1 – unit name; 2 – square grid boundary; 3 – rock fragments (limestone \ dolostone); 4 – sandstone fragments; 5 – bones; 6 – sedimentary structures (laminations). Elevation refers to depth from site datum. (For interpretation of the references to colour in this figure legend, the reader is referred to the web version of this article)
**Figure 4.** Ciota Ciara. Cumulative curves from textural analyses of units 13, 14, 15 and 16. Key: x axis – particle diameter (φ); y axis – cumulative weight percentage. (For interpretation of the references to colour in this figure legend, the reader is referred to the web version of this article)
**Figure 5.** Ciota Ciara. Organic matter content (left) and calcium carbonate content (right) for units 13, 14, 15 and 16.
**Figure 6.** Ciota Ciara. Micrographs of coarse components: (A) subrounded fragment of chert (radiolarite) with clay coating, unit 13, PPL; (B) same as (A) but XPL; (C) rounded pebble of mafic igneous rock ("exotic pebble", see text), unit 14b, PPL; (D) same as (C) but XPL; (E) well-preserved fragment of dolostone; notice strong recrystallization, unit 14f, XPL; (F) probable microlithic flake of chert, unit 14e, XPL, with condenser. (For interpretation of the references to colour in this figure legend, the reader is referred to the web version of this article)
**Figure 7.** Ciota Ciara. Micrographs of components and pedofeatures: (A) weathered bone fragment, with continuous Fe-Mn oxide coating, unit 13, PPL; (B) same as (A) but XPL; (C) rounded phosphatic feature (most probably an excrement); notice also the deformed and fragmented clay coating and the burnt bone fragment with discontinuous Fe-Mn oxide coating, unit14e, PPL (top) and XPL (bottom); (D) same as (C) but fluorescence BL; (E) limpid clay intercalation over laminated sand layer, 14b, PPL; (F) same as (E) but XPL. (For interpretation of the references to colour in this figure legend, the reader is referred to the web version of this article)
**Figure 8.** Ciota Ciara. Micrographs of pedofeatures: (A) groundmass with deformed impregnative nodules of Fe-Mn oxide, unit 14a, PPL (top) and XPL (bottom); (B) phosphatized digested bone fragment with discontinuous Fe-Mn oxide coating, 14e, PPL (top) and fluorescence UV (bottom); (C) phosphatic coating ('rind') on dolostone fragment, unit 14b, PPL; (D) same as (C) but fluorescence BL; (E) silty clay coating and loose discontinuous infilling in channel, 14f, PPL; (F) same as (E) but XPL. (For interpretation of the references to colour in this figure legend, the reader is referred to the web version of this article)
**Figure 9.** Ciota Ciara. Micrographs from unit 15: (A) PPL scan of thin section MFCC-05 (size 95 mm × 55 mm); (B) detail of banded \ platy microstructure, unit 15, PPL (top) and XPL (bottom); (C) silt capping on chert sand grain, unit 15, PPL (top) and XPL (bottom); (D) microlaminated reworked clay coating ('papule'), unit 15, PPL with condenser; (E) same as (D) but XPL with condenser. (For interpretation of the references to colour in this figure legend, the reader is referred to the web version of this article)
**Figure 10.** Ciota Ciara. Presence and development of Fe-Mn oxide coatings: relationships with the bone size (left) and with the weathering degree (right), for units 13, 14 and 15. In both charts, colour shading shows the occurrence and development of Fe-Mn coatings on the bone surface (classed as: absent, less than 50%, more than 50%); in the left graphs, circles correspond to size-classes (between 60 and 500 μm, and larger than 500 μm); in the right graphs, circles correspond to the weathering degree (scaled as: absent, low, intense). See text for details. (For interpretation of the references to colour in this figure legend, the reader is referred to the web version of this article)

**Table I.** Ciota Ciara. List and number of analysed samples (see text for details). Key: TS –thin sections.

| *Unit* | *Grain size* | *Org. matter* | *$CaCO_3$* | *TS* |
|---|---|---|---|---|
| **13** | 3 | 3 | 3 | 1 (C06) |
| **14a** | 1 | 1 | 1 | 2 (C01, C07) |
| **14b** | 4 | 4 | 4 | 1 (C03) |
| **14c** | 2 | 2 | 2 | 1 (C02) |
| **14f\g** | 1 | 1 | 1 | 1 (C08) |
| **14e** | 1 | 1 | 1 | 1 (C04) |
| **15** | 2 | 2 | 2 | 1 (C05) |
| **16** | 1 | 1 | 1 | (none) |

| **Table II.** Ciota Ciara. Main characteristics of excavated units. Key: DP – distribution pattern; fr(s). – fragment(s); OP – orientation pattern. | |
|---|---|
| *Unit* | *Description* |
| **13** | Silty-clay; 7.5YR 5/5, with horizontal black Fe-Mn oxide mottles and nodules; very few dolostone frs. (max. 3 cm, strongly weathered), porosity very low; slightly organic; lower boundary gradual. |
| **14a** | Silty-loam; 6YR 4/6 with Fe-Mn oxide mottles; common dolostone frs. (from mm- to 6 cm-sized), very few sandstone frs.; stones show random DP and OP; few bone frs., porosity very low. |
| **14b** | Silty-loam; 6.5YR 4/5; common dolostone frs. (max. 7 cm), mostly weathered, often with parallel OP in the lower part; the matrix shows same characteristics as 14a; few clay and Mn coating. |
| **14c** | Set of thin intercalations of fine sediment without stones, massive, without visible porosity; from top to bottom: silt, 8YR 6/6, massive; intercalation of Fe-Mn oxide; very fine to medium sand layer, 6YR 6/6 (4 cm-thick); thin discontinuous silty-sand level, 7.5YR 6/6. |
| **14f\g** | Silty-loam; common dolostone frs. (cm-sized, mostly moderately weathered); matrix similar to 14b, 6.5YR 4/6; lower boundary clear. |
| **14e** | Clast-supported breccia composed of dominant dolostone frs. (max. 20 cm) and very few sandstone frs.; stones show OP parallel to the unit interface; silty-loam matrix; 6.5YR 4/6; common clay and Fe-Mn coatings, mostly on stones. |
| **15** | Clast-supported breccia composed of dolostone frs. (dm-sized on average, with slight variation of size from top to bottom – larger stones on top); silty-loam matrix; 5YR 4/4; lower boundary clear. |
| **16** | Clast-supported breccia composed of dm-sized dolostone frs.; silty-loam matrix; 5YR 4/4; lower boundary sharp to bedrock. |

**Table III**. Ciota Ciara. Main micromorphological characteristics (I): microstructure and components. Key: dev. – developed; fr(s). – fragment(s); mod. – moderately; coarse components are reported in order of abundance (see text for details).

| Unit | Microstructure \ aggregation | Porosity | Coarse Components | Fine Material |
|---|---|---|---|---|
| 13 | Subangular blocky, weakly dev.; locally spongy | Common deformed weakly accommodated planes; few channels; very few vughs | Common SIL (quartz, chert, feldspars and micas) and CRB (calcite/dolomite and dolostone frs.); few ABC (bone frs. and phosphates, very few charcoal frs.) | Brown, speckled |
| 14a | Subangular blocky, weakly dev. and separated; locally channel | Few planes, weakly accommodated, channels, chambers and vughs | Common SIL (quartz, chert, feldspars, and micas) and CRB (calcite/dolomite and dolostone frs.); few ABC (bone frs. and excrements) | Brown, speckled |
| 14b (top) | Subangular blocky, mod. dev. and weakly separated | Common planes, mod. accommodated; very few vughs | Common SIL (quartz and chert, few sandstone and micas) and CRB (calcite/dolomite and dolostone frs.); few ABC (bone frs., few phosphates and charcoal frs.) | Brown, speckled |
| 14b (bottom) | Subangular blocky, weakly dev. and separated | Common planes, mod. accommodated; very few vughs | Common SIL (quartz, chert and micas, very few mafic rock frs.) and CRB (calcite/dolomite and dolostone frs.); few ABC (bone frs., few phosphates and charcoal frs.) | Brown, speckled |
| 14c | Single- to bridged-grain | Complex packing voids | Frequent SIL (quartz and chert, common feldspar and micas) | Yellowish brown, speckled |
| 14f (top) | Platy, mod. to well separated and dev. | Few planes, mod. to well accommodated, parallel to the unit interface | Common SIL (quartz, chert, feldspars, and micas) and CRB (calcite/dolomite and dolostone frs.); few ABC (bone frs. and phosphates) | Brown, speckled and dotted |
| 14f (bottom) | Platy, well separated and well dev. | Very few planes, mod. accommodated, parallel to the unit interface, very few channels, very few vesicles | Common SIL (quartz, chert, feldspars, and micas) and CRB (calcite/dolomite and dolostone frs.); few ABC (bone frs. and phosphates) | Brown, speckled and dotted |
| 14e | Platy, well separated and well dev. | Few planes, moderately accommodated, oblique to the unit interface; very few channels and chambers; few vughs | Common SIL (quartz, chert, plagioclase and micas, few sandstone) and CRB (calcite/dolomite and dolostone frs.); few ABC (bone frs., phosphates and excrements) | Speckled and dotted |
| 15 | Platy, well separated and well dev. | Few well accommodated planes, few vughs and vesicles | Common SIL (quartz, chert, feldspars, and micas) and CRB (calcite/dolomite and dolostone frs.); few ABC (bone frs. and phosphates) | Brown, limpid |

**Table IV**. Ciota Ciara. Main micromorphological characteristics (II): groundmass and pedofeatures. Key: c/f RlDP – coarse/fine related distribution pattern; fr(s). – fragment(s); undiff. – undifferentiated.

| Unit | c/f RlDP | b-fabric | Pedofeatures and Sedimentary Features |
|---|---|---|---|
| 13 | Single to double-spaced and open porphyric | Speckled, locally weakly dev. granostriated | Few dusty-clay coatings on voids associated with Fe-Mn hypocoatings; few clay coatings around grains; few impregnative black Mn-Fe nodules; few Mn coatings and hypocoatings around bone frs; few phosphatic nodules; few infillings of amorphous phosphates |
| 14a | Single to double-spaced porphyric | Undiff., locally monostriated and granostriated | Few loose discontinuous infillings; few dusty-clay coatings on grains and rock frs.; few deformed clay coatings; few typic impregnative black Mn-Fe nodules; few Mn coatings and hypocoatings around bone frs.; very few phosphatic nodules |
| 14b (top) | Single to double-spaced porphyric | Undiff., locally granostriated | Common typic impregnative black Fe-Mn nodules; few deformed clay coatings; few phosphatic rinds; very few clay intercalations |
| 14b (bottom) | Single to double-spaced porphyric | Undiff., locally granostriated | Common impregnative black Mn-Fe nodules; few deformed clay coatings; few clay intercalations; few phosphatic rinds; very few dusty-clay coatings on voids |
| 14c | Chitonic to gefuric | Granostriated | Few clay papules; few typic and dendritic impregnative Fe-Mn nodules; clay depletion |
| 14f (top) | Single to double space porphyric | Undiff., weakly dev. granostriated | Few deformed clay coatings; few dusty-clay coatings on voids; few impregnative black Mn-Fe nodules; few Fe-Mn coatings on bone frs.; few loose discontinuous infillings; few phosphatic nodules; very few phosphatic rinds; very few dusty-clay coatings on voids; very few poorly dev. cappings on rock frs. |
| 14f (bottom) | Single to double space porphyric | Undiff., weakly dev. granostriated, locally speckled | Few deformed and fragmented clay coatings; few impregnative black Mn-Fe nodules; few Mn-Fe hypocoatings on bone frs.; few phosphatic nodules; very few phosphatic rinds, very few clay papules |
| 14e | Single to double space porphyric | Undiff., locally granostriated | Common deformed and fragmented clay coatings; few impregnative black Mn-Fe nodules; few loose discontinuous infillings; few phosphatic rinds; very few clay papules |
| 15 | Close porphyric, locally gefuric | Granostriated, locally undiff. | Common dusty-clay cappings on rock frs.; common clay papules; common phosphatic coatings and nodules; few dusty-clay coatings around grains; few impregnative black Mn-Fe nodules |

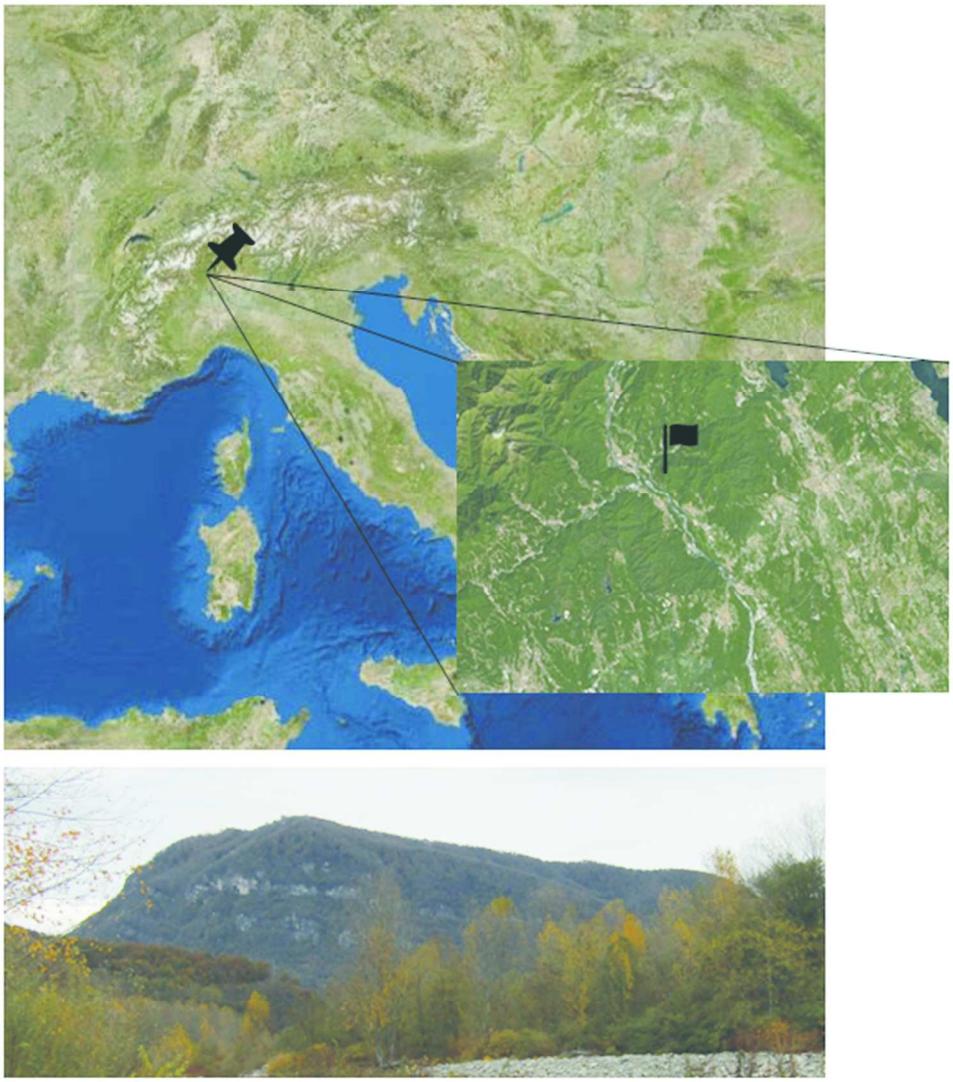

Figure 1. Location (above) and view of Monte Fenera (below).

160x178mm (300 x 300 DPI)


Figure 2. Ciota Ciara. Top right: sketch plan of the cave: solid line – outline of the cave wall; dashed line – dripline at the cave entrances; 1 – W entrance (the "window"); 2 – SW entrance in 2009 (before excavation). Bottom right: long-section of the cave (modified after Fedele, 1966).

238x150mm (300 x 300 DPI)

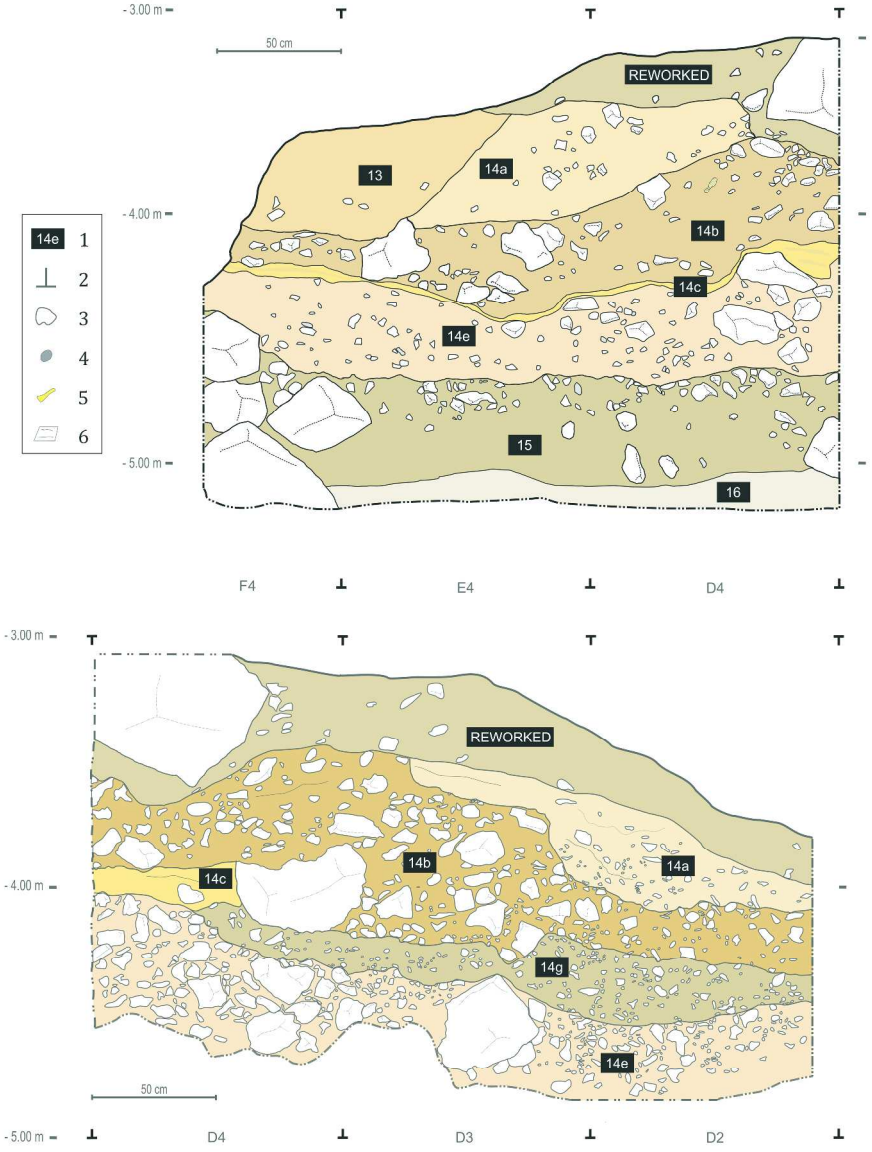


Figure 3. Ciota Ciara. Stratigraphic cross-sections across squares F4-D4 (top) and D4-D2. Key: 1 – unit name; 2 – square grid boundary; 3 – rock fragments (limestone \ dolostone); 4 – sandstone fragments; 5 – bones; 6 – sedimentary structures (laminations). Elevation refers to depth from site datum. (For interpretation of the references to colour in this figure legend, the reader is referred to the web version of this article)

304x394mm (300 x 300 DPI)

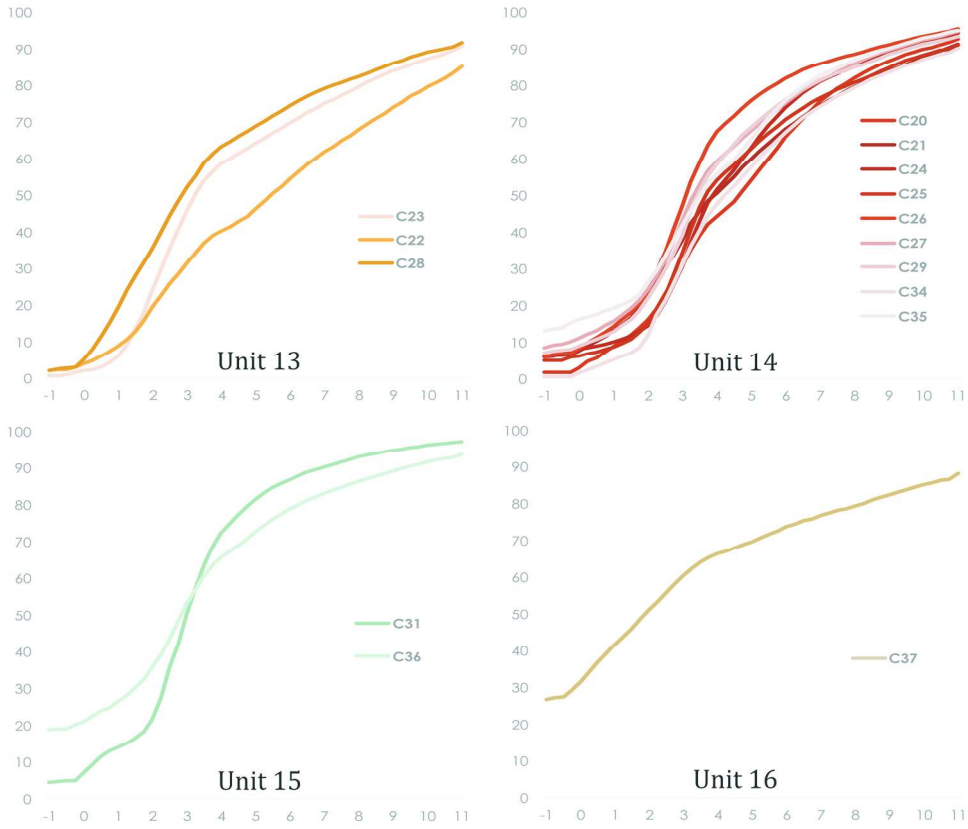


Figure 4. Ciota Ciara. Cumulative curves from textural analyses of units 13, 14, 15 and 16. Key: x axis – particle diameter (φ); y axis – cumulative weight percentage. (For interpretation of the references to colour in this figure legend, the reader is referred to the web version of this article)

183x159mm (300 x 300 DPI)


Figure 5. Ciota Ciara. Organic matter content (left) and calcium carbonate content (right) for units 13, 14, 15 and 16.

200x200mm (300 x 300 DPI)

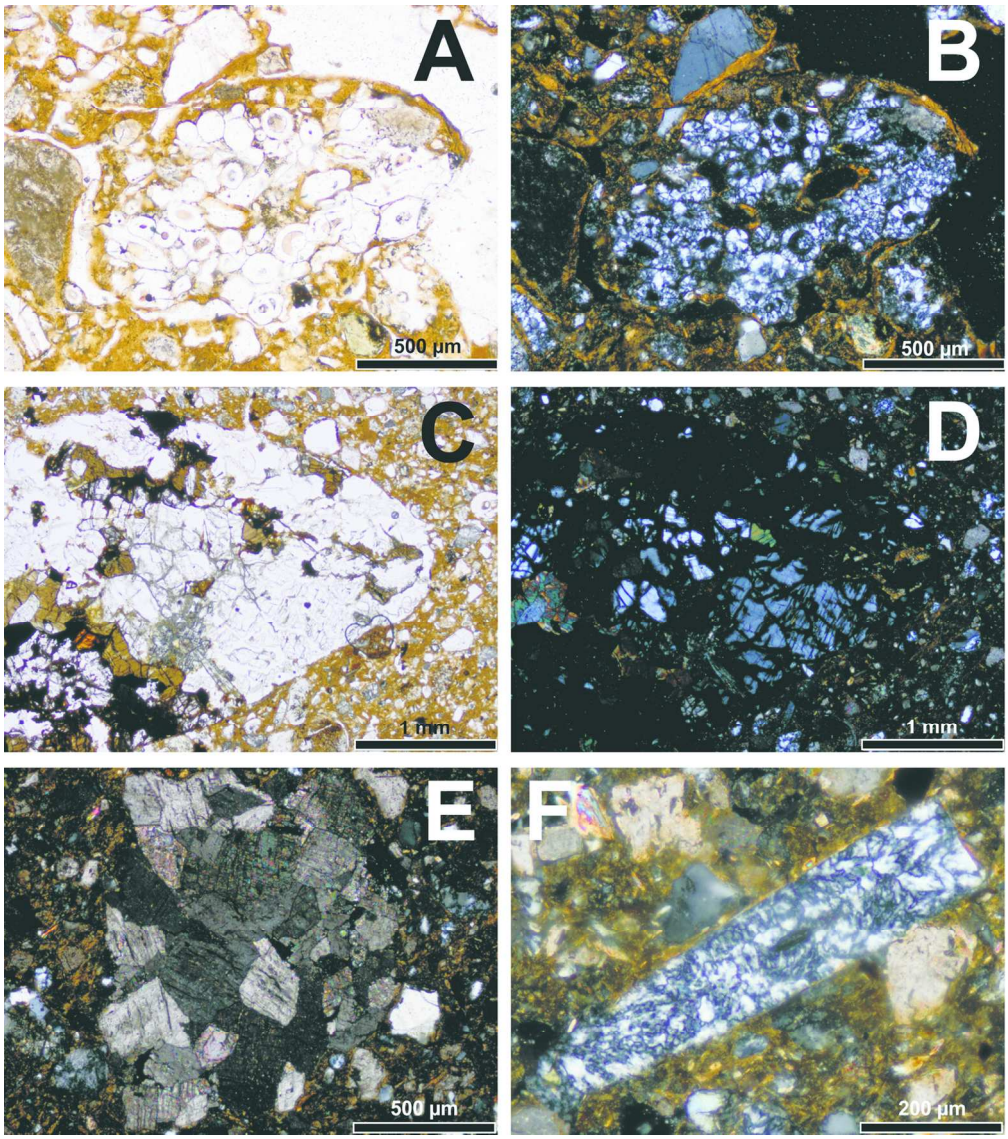


Figure 6. Ciota Ciara. Micrographs of coarse components: (A) subrounded fragment of chert (radiolarite) with clay coating, unit 13, PPL; (B) same as (A) but XPL; (C) rounded pebble of mafic igneous rock ("exotic pebble", see text), unit 14b, PPL; (D) same as (C) but XPL; (E) well-preserved fragment of dolostone; notice strong recrystallization, unit 14f, XPL; (F) probable microlithic flake of chert, unit 14e, XPL, with condenser. (For interpretation of the references to colour in this figure legend, the reader is referred to the web version of this article)

137x154mm (300 x 300 DPI)

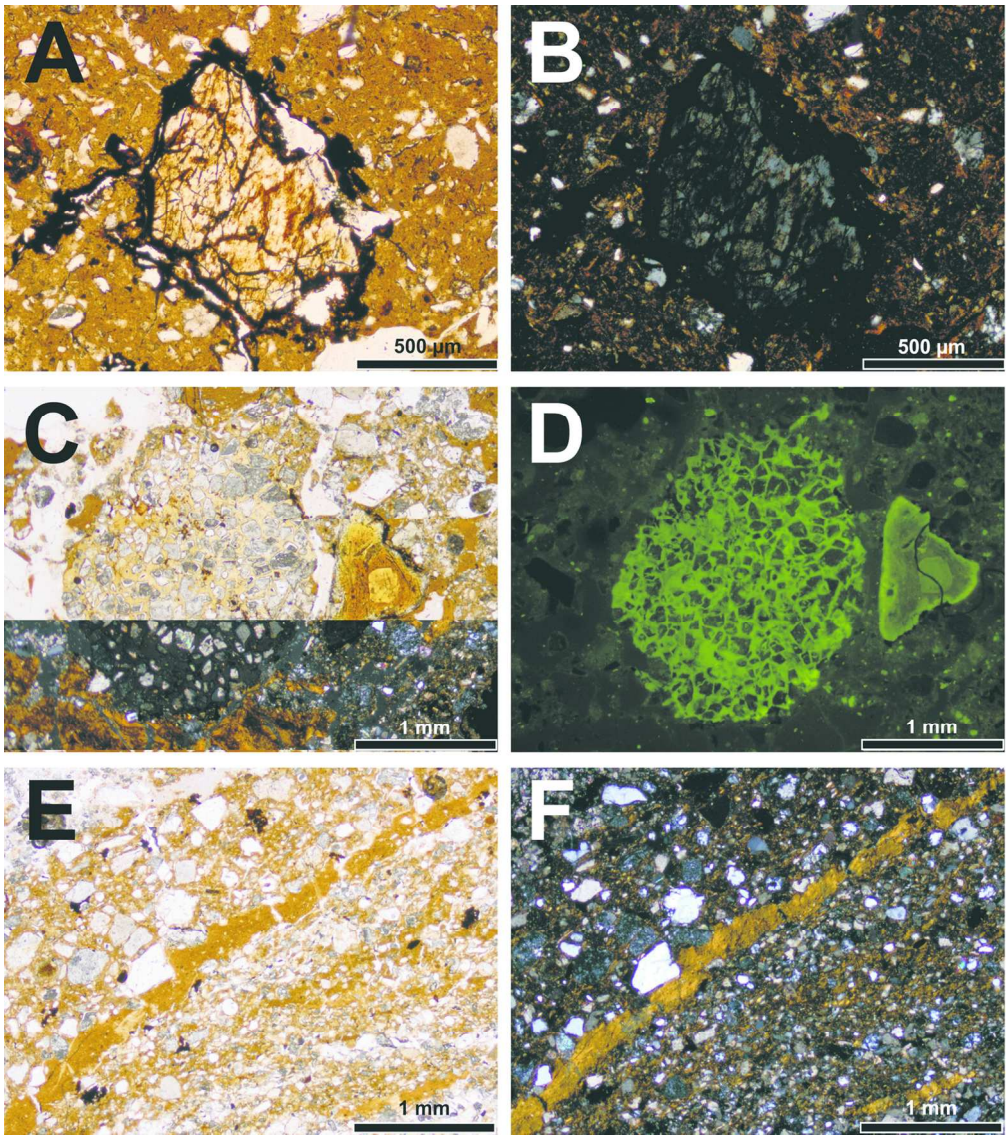


Figure 7. Ciota Ciara. Micrographs of components and pedofeatures: (A) weathered bone fragment, with continuous Fe-Mn oxide coating, unit 13, PPL; (B) same as (A) but XPL; (C) rounded phosphatic feature (most probably an excrement); notice also the deformed and fragmented clay coating and the burnt bone fragment with discontinuous Fe-Mn oxide coating, unit14e, PPL (top) and XPL (bottom); (D) same as (C) but fluorescence BL; (E) limpid clay intercalation over laminated sand layer, 14b, PPL; (F) same as (E) but XPL. (For interpretation of the references to colour in this figure legend, the reader is referred to the web version of this article)

137x154mm (300 x 300 DPI)

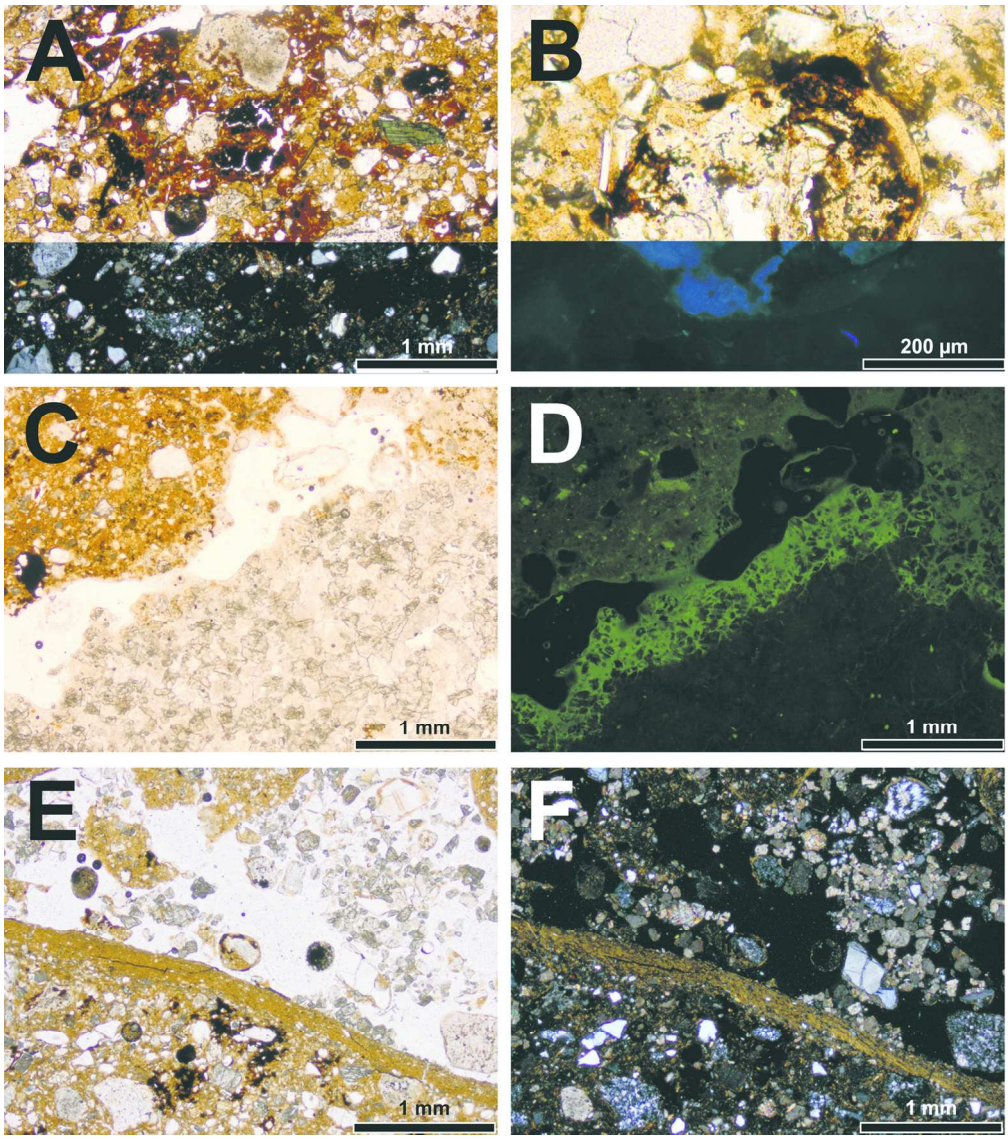


Figure 8. Ciota Ciara. Micrographs of pedofeatures: (A) groundmass with deformed impregnative nodules of Fe-Mn oxide, unit 14a, PPL (top) and XPL (bottom); (B) phosphatized digested bone fragment with discontinuous Fe-Mn oxide coating, 14e, PPL (top) and fluorescence UV (bottom); (C) phosphatic coating ('rind') on dolostone fragment, unit 14b, PPL; (D) same as (C) but fluorescence BL; (E) silty clay coating and loose discontinuous infilling in channel, 14f, PPL; (F) same as (E) but XPL. (For interpretation of the references to colour in this figure legend, the reader is referred to the web version of this article)

137x154mm (300 x 300 DPI)

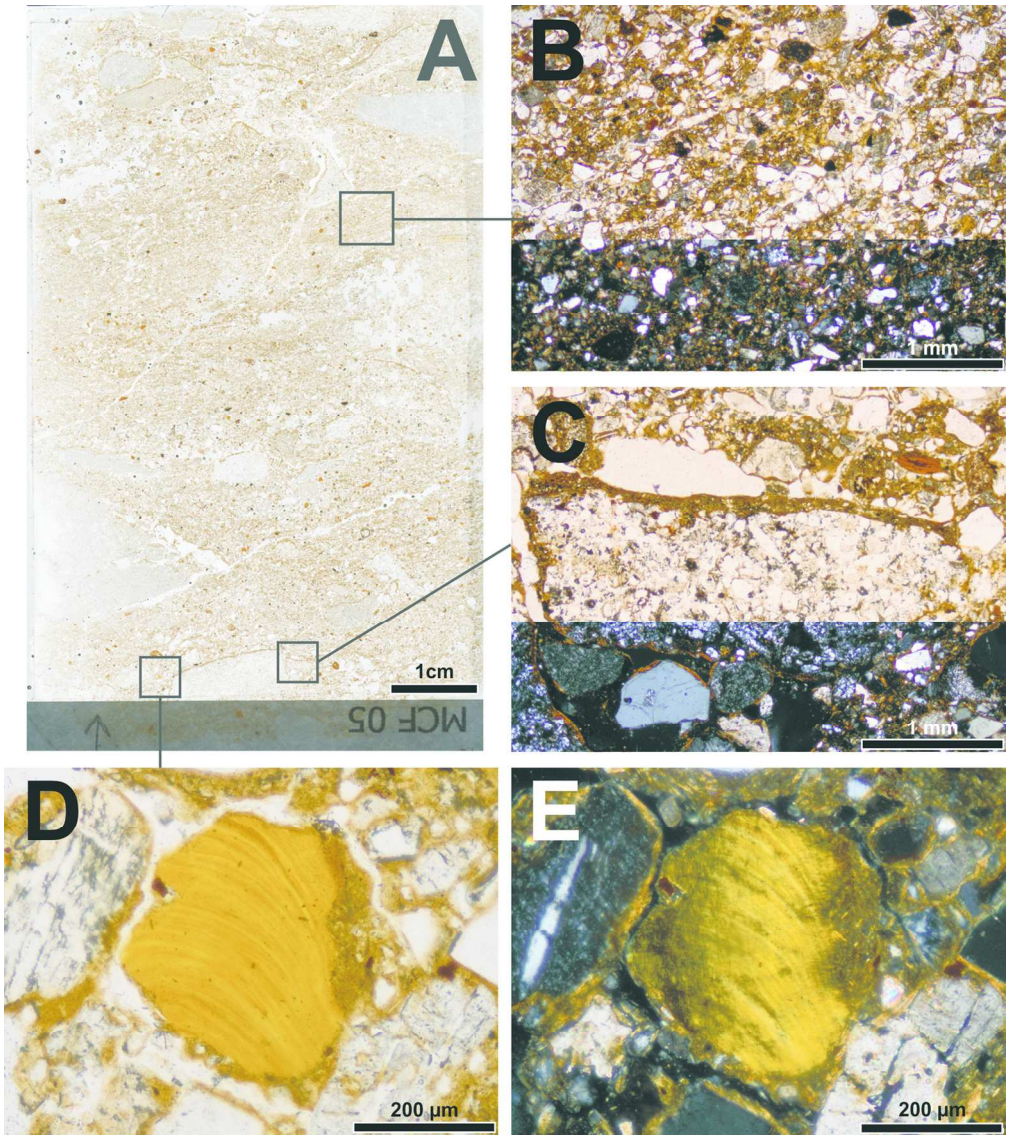


Figure 9. Ciota Ciara. Micrographs from unit 15: (A) PPL scan of thin section MFCC-05 (size 95 mm × 55 mm); (B) detail of banded \ platy microstructure, unit 15, PPL (top) and XPL (bottom); (C) silt capping on chert sand grain, unit 15, PPL (top) and XPL (bottom); (D) microlaminated reworked clay coating ('papule'), unit 15, PPL with condenser; (E) same as (D) but XPL with condenser. (For interpretation of the references to colour in this figure legend, the reader is referred to the web version of this article)

137x155mm (300 x 300 DPI)


Figure 10. Ciota Ciara. Presence and development of Fe-Mn oxide coatings: relationships with the bone size (left) and with the weathering degree (right), for units 13, 14 and 15. In both charts, colour shading shows the occurrence and development of Fe-Mn coatings on the bone surface (classed as: absent, less than 50%, more than 50%); in the left graphs, circles correspond to size-classes (between 60 and 500 µm, and larger than 500 µm); in the right graphs, circles correspond to the weathering degree (scaled as: absent, low, intense). See text for details. (For interpretation of the references to colour in this figure legend, the reader is referred to the web version of this article)

266x383mm (300 x 300 DPI)